Seismic Retrofit of a Concrete Framed High-Rise Historic Building Using Supplementary Damping

Lon M. Determan, S.E., Principal
Amir S. J. Gilani, PhD., S.E., Expert Structural Specialist
H. Kit Miyamoto, M.S., S.E., President & CEO
Miyamoto International, Inc.
Structural and Earthquake Engineers
West Sacramento, CA

Abstract

Fluid viscous dampers were used to retrofit a historic high-rise building in Sacramento, California. The building was constructed in the 1920's and was the first high-rise constructed in the state capital. It has 14 stories and a full basement. The building is also a state registered historic structure, and has many unique architectural features such as terra cotta tile veneer. Reinforced concrete moment frames throughout the height and reinforced concrete structural walls at the lower two floors comprise the lateral-load resisting system of this building. As part of the city's downtown revitalization, this historic structure is being transformed from an office building into a premier boutique hotel. Due to this change of occupancy, the building must now satisfy both Life Safety and Collapse Prevention performance objectives at design and ultimate earthquakes, respectively. Performance-based earthquake engineering revealed that the building would experience story drifts at its middle stories. At these levels, the concrete beams had unacceptable plastic hinge rotations. These drifts could potentially cause damage to both structural and historic non-structural components. Fluid viscous dampers were added to these critical stories to mitigate this deficiency. Additionally, steel bracing was added at the first floor to provide additional lateral and torsional stiffness and mitigate the effect of full-length reinforced concrete walls on the two back faces of the building. Analyses of the retrofitted building indicated that the performance was improved and it met its seismic performance goals.

Introduction

Fluid Viscous Dampers (FVDs) provide an optimal method for retrofitting historic and essential facilities. Due to the significance of these facilities, these structures must be preserved and need to meet seismic performance requirements during earthquakes. A brief discussion of FVDs is presented below. It is followed by application of these devices for seismic retrofit of a multi-story reinforced concrete building.

Fluid Viscous dampers

FVDs provide an effective and economical method for retrofit of reinforced concrete structures. They are external devices, originally developed for shock and vibration control in the defense and aerospace industries. In the past decade, they have been used for seismic protection in both retrofit and new construction for many structures including reinforced concrete buildings. FVDs consist of a cylinder and a stainless steel piston. The cylinder is filled with incompressible silicone fluid that has stable properties over a wide range of operating temperatures. FVDs are activated by the transfer of the silicone fluid between chambers at opposite ends of the unit through small orifices. The mechanical construction and orifice properties can be varied to obtain the desirable damper properties. Figure 1a presents the cross section of a typical FVD device, whereas; Figure 1b shows one of the actual devices that will be used for the building described in this paper.

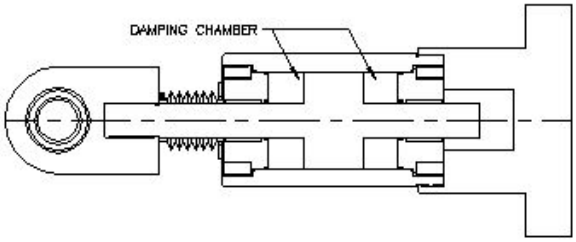

a. FVD cross section

b. Photograph of FVD

Figure 1. Schematic and photograph of FVD

For seismic applications, FVDs are attached parallel to frames in or near parts of the structure that experience large relative displacements. They are incorporated in braces and placed in various configurations in individual bays. The force-velocity relation for our FVD is computed as:

$$F = C\,\mathrm{sgn}(V)V^{\alpha} \qquad (1)$$

where, F and V are the damper force and velocity, respectively, C is the effective damping coefficient, and α is the damper exponent. FVDs are installed in series with HSS sections with stiffness K, and attached to existing or new beam and column elements. Dampers have elastic and viscous components in series. The stiffness of the damper unit itself is much larger than that of the connecting brace element. They are modeled as Maxwell viscoelastic elements. The effect of parameters K and α on the hysteretic response of the damper are depicted in Figure 2 for a constant value of C. For purely viscous behavior, α equals unity and K is large. This case gives the largest dissipated energy per cycle and imparts no additional forces into the structure because the FVD force is 90 degrees out-of-phase with the elastic forces. This corresponds to a linear FVD design. However, such design could result in large damper force and would require large connections to resist such a force. Alternatively, nonlinear dampers with α less than unity can be used. By increasing the parameter C, nonlinear dampers will dissipate similar energy as linear dampers but with smaller damper forces. The component of force in-phase with elastic forces is also small for nonlinear dampers. The FVD efficiency is maximized as K is increased.

As shown in Figure 2, the devices dissipate energy, which increases the effective damping of the building. The plots are shown for both linear and nonlinear dampers. FVDs do not increase the building stiffness and hence do not attract more seismic forces. Hence, they reduce story drifts and demand on existing members without substantially increasing demand on columns and foundations. During seismic events, the devices become active and the seismic input energy is used to heat the fluid and is thus dissipated. FVDs have been extensively researched [2] and implemented in the upgrade of many structures. The authors have used this retrofit method for the seismic retrofit of other historic non-ductile concrete structures; see [6]. FEMA 356 [5] requires prototype testing of FVDs to verify that the force-displacement relation and damping coefficients used in analysis can be accurately replicated in the field. Prototype testing of FVDs, used in the retrofit of subject building was performed at the manufacturer's laboratory [Taylor, 2006]. Testing included endurance cyclic tests, seismic tests at the design displacements, and tests at elevated temperatures. Sample force-history and force-velocity data are shown in Figure 3.

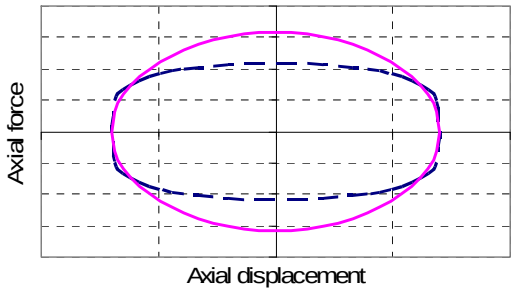

a. Solid (α=1), dashed α=0.5)

Figure 2. Hysteretic response of FVD for one full cycle of sinusoidal loading

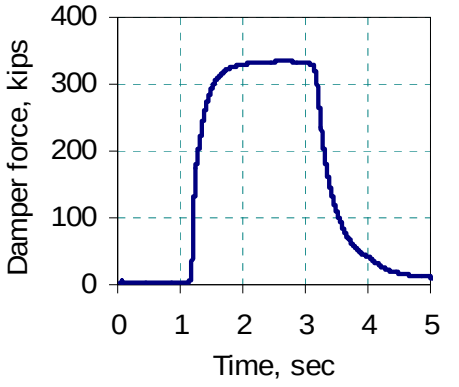

a. Force history

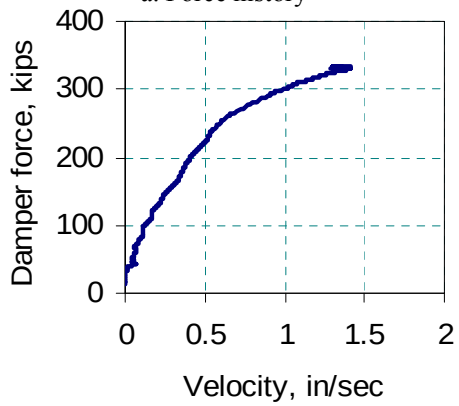

b. Force-velocity relation

Figure 3. Hysteretic response of FVD

Description of the high-rise structure

Subject building is 200 ft (61 m) tall and has 14 stories and a full basement. It is located at the corners of 10th and J Streets in downtown Sacramento, California. It was constructed in 1922 as the first high-rise building constructed in the city. Full-length perimeter walls span between the ground floors and the basement. The footprint for the original construction was L-shaped, measuring 80 x 120 ft (24 x 36 m) with a total area of approximately 70,000 ft^2 (6,500 m^2). Two later additions to the buildings were a 6-story, 23,000 ft^2 (2,100 m^2) annex in 1932, and a 2-story L-shaped annex in 1950. Figure 4 presents a photograph of the building. As seen in Figure 4, the building has many unique architectural features, including a terra cotta skin on the perimeter. Because of its many unique features, this building is considered a historic structure that must be preserved.

The gravity load-resisting system consists of 5- and 6-in. (125- and 150-mm) thick reinforced concrete one-way slabs supported on reinforced concrete beams and columns. Reinforced concrete moment frames resist lateral loading. Additionally, between first and second floors, 8-in. (200-mm) thick reinforced concrete walls span the entire length on two faces. Reinforced concrete walls extended approximately half of length on two faces, between the second and third floors. At the lower levels, the concrete columns measure 24 in. (600 mm) square, and are reinforced with up to twenty 1-1/8 in. (29 mm) square bars. The transverse reinforcement for columns is 3/8 in. (9 mm) diameter bars at 4-in. (10-mm) spacing. Smaller column sizes and reinforcement are used at upper floors. A variety of beam sizes were used in the building. Typical beams measure 10 x 24 in. (250 x 600 mm) and are reinforced with two ¾- in. (19 mm) square bars at top and bottom. ½-in. (13 mm) diameter stirrups are used as beam ties. Deep spandrel beams up to 43 in. (1,100 mm) deep occur along the perimeter at the lower levels. Figure 5 presents the typical floor plans for the building.

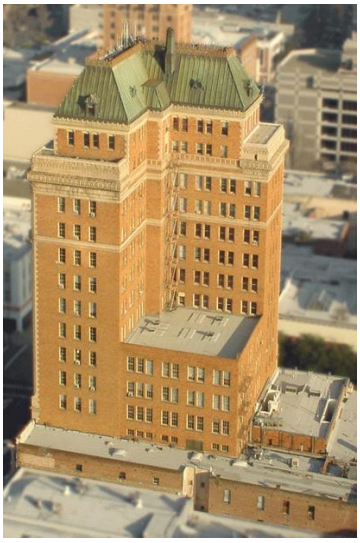

a. Looking East

Figure 4. Photograph of the building

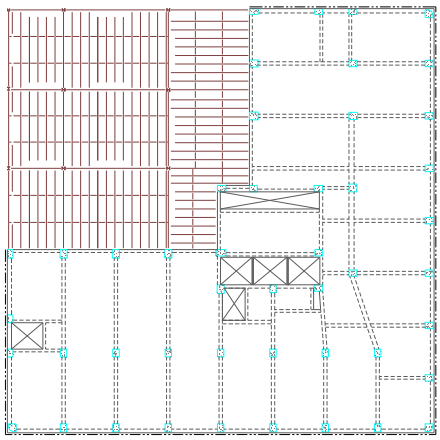

a. Third floor

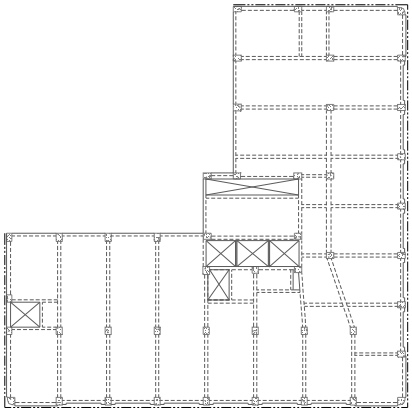

b. Eighth floor

Figure 5. Building typical floor plans

Performance Objectives

The building was originally designed as a mixed-use facility. In 2004, the owner decided to evaluate and undertake seismic evaluation of the building for use of California state government tenancy. This implied a one-level occupancy upgrade and the building had to meet the Life Safety (LS) performance for the Design Basis Earthquake (DBE). In 2006, it was decided to convert the building to a hotel. Since this meant a two-step upgrade in occupancy, the building now also had to meet Collapse Prevention (CP) for the Maximum Credible Event (MCE). These two performance objectives—LS at DBE level and CP at MCE level—were used in evaluations presented hereafter.

Seismic Demand

A geotechnical site investigation [7] was conducted to determine the site-specific acceleration spectra for this building. Both the DBE spectra (10% probability of exceedence in 50 years, or 475-year return period) and MCE spectra (2% probably of exceedence in 50 years or 2,500-year return period) were developed based on the site geological evaluation, proximity of active faults, and historic seismic activities. Figure 6 presents the DBE and MCE response spectra.

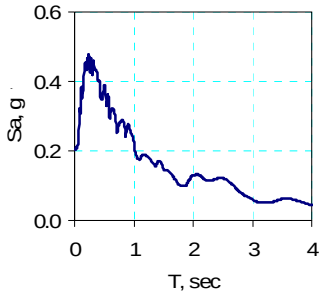

a. DBE

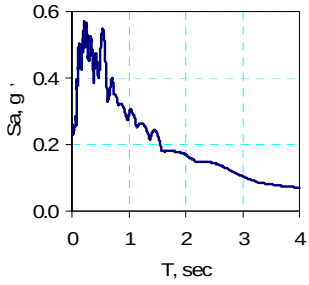

b. MCE

Figure 6. Seismic demand

Three sets of time histories were prepared to match each of the two spectra. The acceleration seeds were taken from the 1989 Loma Prieta earthquake. Figure 7 shows the two acceleration spectra used in analysis and a 20-sec trace of one of the horizontal components of one of the acceleration records for each level. The DBE and MCE spectra are anchored at 0.2 and 0.25 g and have maximum spectral accelerations of 0.44 and 0.57 g, respectively.

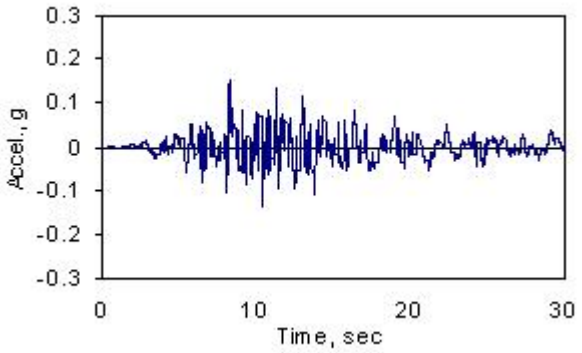

a. DBE

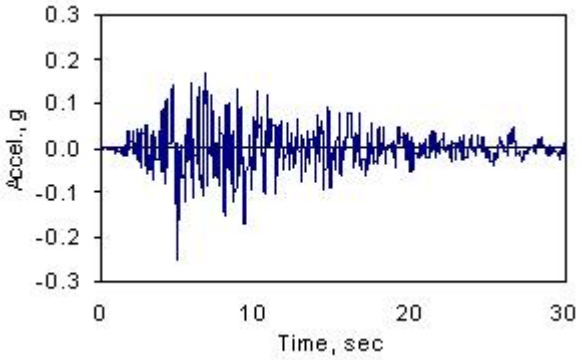

b. MCE

Figure 7. Typical acceleration traces

Response of the Existing Building

Computer programs ETABS [3] and SAP 2000 [4] were used to prepare mathematical models of the building. All pertinent stiffness and mass components were included in the model. Compressive strengths of 5.2 and 4.6 ksi (39 and 32 MPa) were obtained for concrete columns and beams, respectively from material samples tested by Wallace-Kuhl [9]. Nominal properties of Grade 40 (275 MPa) steel were used for reinforcement. Nominal dimensions, as shown in contract plans were used in analysis. Member sizes and spans were verified during site visits. Beam-to-column connections were modeled as rigid. Concrete floor slabs were modeled as shell elements and rigid diaphragms were applied to them. Member plastic hinge properties were derived using the FEMA 356 [4] recommendations. Conservatively, the stiffness contribution from the unreinforced masonry (URM) infills was ignored—and equivalent struts were not included in the model because multiple windows perforate these infills; see Figure 4. The inertial weight of the building is estimated at 23,000 kips (100 MN).

Table 1 presents the modal properties of the building for the first six modes. In analysis, 18 modes were used to ensure that over 90% mass participation of the structure was accounted for. Note that the fundamental mode has a period of approximately 2.1 to 2.2 sec, the modes are uncoupled, and nearly 60% of the total mass participates in the first mode.

		Mass participation, %		
Mode	Period, sec	x-	y-	θ-
1	2.2	59	4	6
2	2.1	4	58	3
3	1.9	1	2	54
4	0.8	12	3	1
5	0.8	2	11	0
6	0.7	0	0	11

Table 1. Modal properties

The building was subjected to the response spectrum loading of Figure 6 and its response was evaluated. Analysis indicated that the building did not exhibit any irregular response; there was neither soft story response, nor, amplified torsional behavior. Figure 8 presents the displaced shape of the exterior frame subjected to response spectral loading in the x- (N-S) direction. Note that the maximum story drifts occur near the mid-height of the building, between fourth and eighth floors. Although, the story drifts are not excessive at these levels, they could potentially cause damage to the existing nonstructural elements, including the terra cotta and URM infill at these levels.

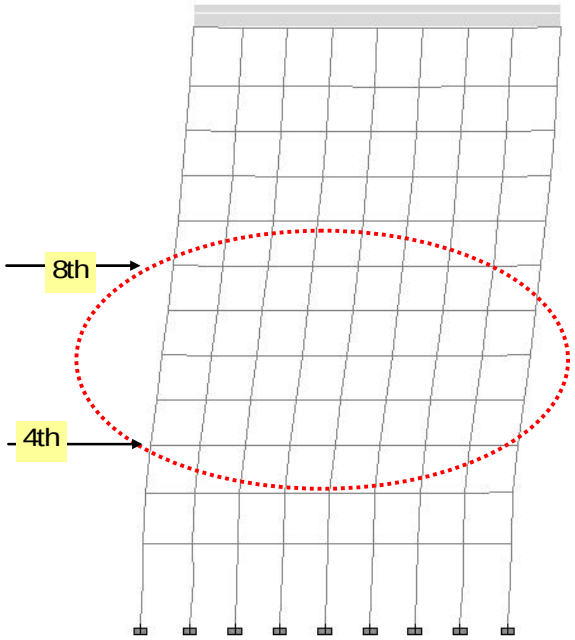

Figure 8. Response spectrum deformation

For regular structures with a dominant first mode response, such as the building under investigation, static nonlinear (pushover) analysis can be used to accurately estimate the seismic response of the building. The control node was selected at approximately the center of mass at the attic level. In each lateral direction, two loading patterns were considered: one resembling the deformed shape obtained from the response spectrum analysis, and the other proportional to the seismic mass at the floors (uniform acceleration). The structure was preloaded with gravity effects, then incrementally displaced to the target displacement computed from nonlinear response history analyses. The concept of equal displacement was utilized. Figure 9 presents the displaced shape of an exterior frame at target displacement of approximately 8 in. (200 mm) at the control node—a value close to the anticipated roof displacement during the DBE event.

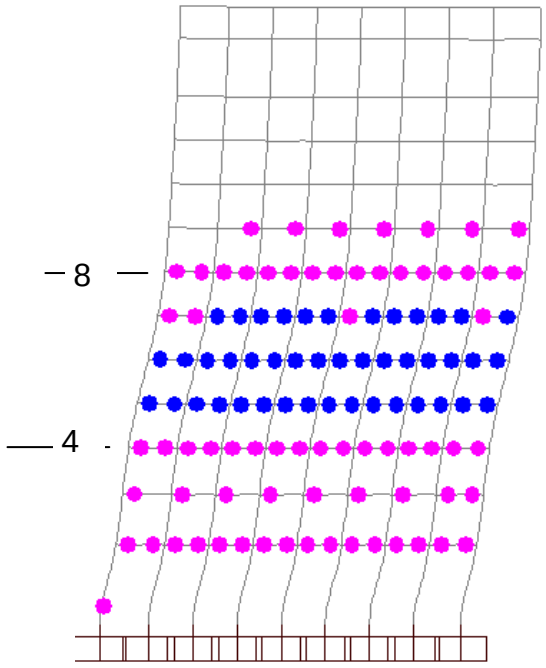

Figure 9. Displaced shape

The building global response is adequate as it meets the LS requirements. However, the largest drifts and plastic hinge rotations occur at the mid-height of the building; see Table 2 results of two-dimensional analysis at the DBE level. The mid-level floors experience large deformations and seismic demand on the concrete beams.

Floor	Drift, %	PH rotation, % radian
Attic	0.18	0
12	0.26	0
11	0.38	0
10	0.54	0
9	0.67	0.03
8	0.73	0.25
7	0.65	0.58
6	0.53	0.79
5	0.47	0.77
4	0.37	0.37
3	0.12	0.05
2	0.13	0.48

Table 2. Story drifts and plastic hinge rotations, DBE level

Principle of Equal Displacement

For regular structures that have large periods and do not experience substantial post-yielding behavior, the principle of equal displacement can be applied. This principle [10] states that, for such structures, the elastic and inelastic displacements are approximately equal. Thus, the inelastic displacement and drifts, but not the member forces or base shear, can be accurately estimated from elastic models. As noted, this building has a long fundamental period and insignificant modal coupling, and, hence, is a candidate for this approach. To ascertain the level of nonlinearity in the building, a two-dimensional model of one of the exterior frames was prepared; see Figure 10. This model was dynamically equivalent to the three-dimensional model because the models had similar modal properties.

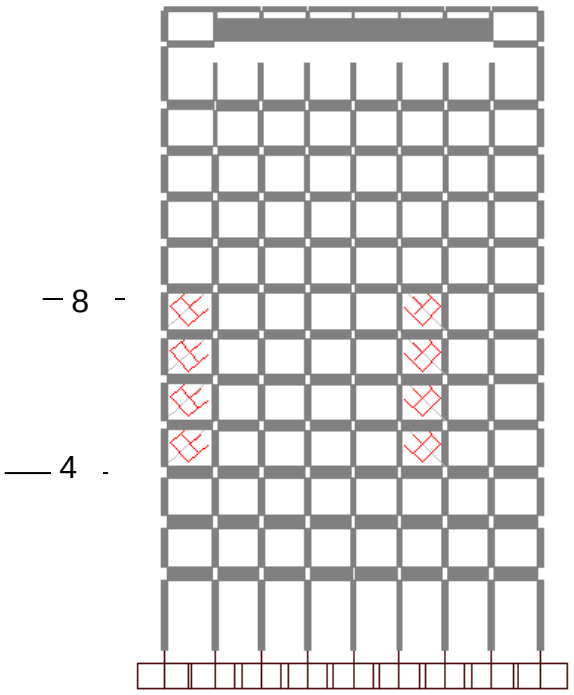

Figure 10. Two-dimensional model of typical frame (elevation)

Two parallel simulations were conducted. In the first analysis, the members were modeled as elastic and only nonlinearity in the FVDs was reproduced. In the second analysis, nonlinear response in both dampers and concrete members were included. The roof displacement histories were contrasted. As shown in Figure 11a, at the DBE level, the models produce identical results because the level of nonlinearity in the concrete members is small. Figure 11b indicates that even at MCE level, the two analyses produce similar results. The maximum displacement is only approximately 10% larger when member nonlinear behavior is modeled (solid line). Therefore, the principle of equal displacement is used for the remainder of the analysis and this paper.

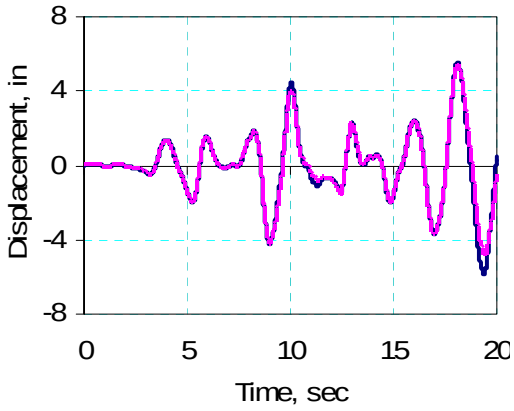

a. DBE roof displacements

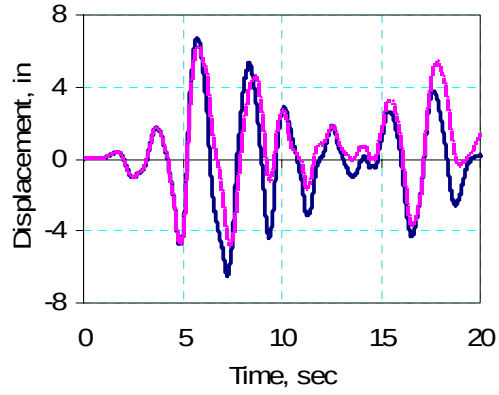

b. MCE roof displacements

Figure 11. Correlation of analyses: including and excluding member nonlinearity

Response of the Retrofitted Building

FVDs, steel braces, and fiber-reinforced polymer (FRP) composites were used in the seismic upgrade. Sixteen FVDs were added between the fourth and eighth floors to reduce story drift ratios and seismic demand on the reinforced concrete members at these levels. Figure 12 presents a schematic of FVD connections to the existing concrete members, and the location of the FVDs.

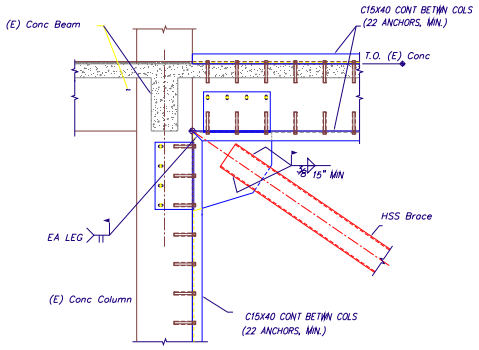

a. Connection detail (elevation)

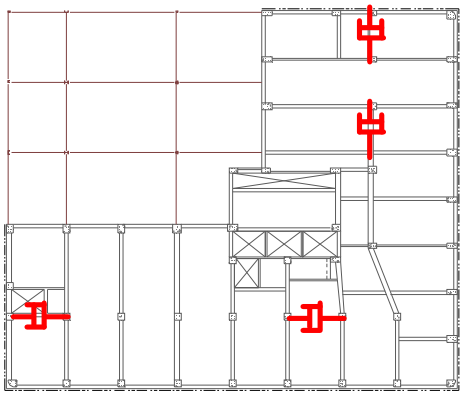

b. Typical location (plan)

Figure 12. Seismic retrofit with FVDs

Diagonal steel HSS braces were added between the first and second floors. These braces were placed opposite the existing 8-in. (200 mm) reinforced concrete wall and were intended to add lateral stiffness and reduce torsional response at this level. FRP was added to the floor slabs to serve as drag struts (collectors) and served to transmit and distribute the seismic forces between the damper bays and the floor diaphragms. The dampers have a velocity exponent (α) of 0.5 and a damping constant (C) equal to 300 kip-sec/in. (8.5 MN-sec/m). The steel connections at the ends of dampers and the components transferring the damper forces to the existing members were designed for the MCE level forces. Since these forces are substantially out-of-phase with elastic forces, they do not significantly increase loading on these existing members.

Nonlinear static and dynamic analyses were performed to assess the seismic response of the retrofitted building at the DBE and MCE levels. The seismic demand on the building was obtained from nonlinear dynamic analyses. Figure 13 presents the x-component of the computed displacements at the attic-level control node.

The DBE displacement equals 8 in. (200 mm). The capacity of the building to sustain such displacements was computed from static nonlinear analysis. As shown in Figure 13b, the building meets its LS goal at the DBE level.

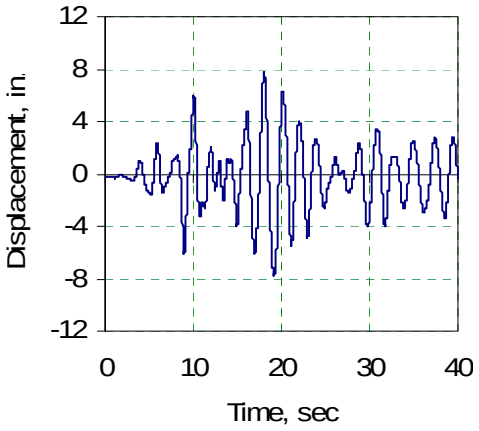

a. Displacement response

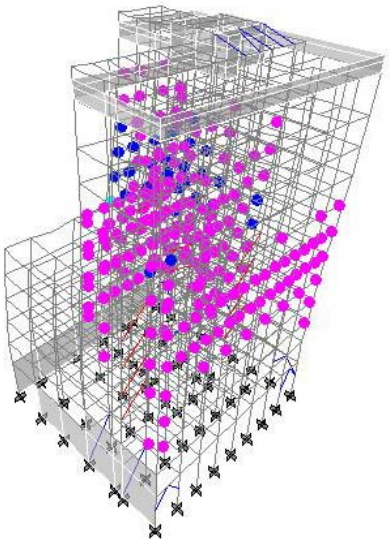

b. performance

Figure 13. Seismic demand and capacity, DBE level

The MCE design displacement is computed as 11 in. (280 mm). Figure 14 shows the displaced shape of the building at the MCE displacement and the hinges formed at this level. The structure meets its CP performance goal at the MCE level.

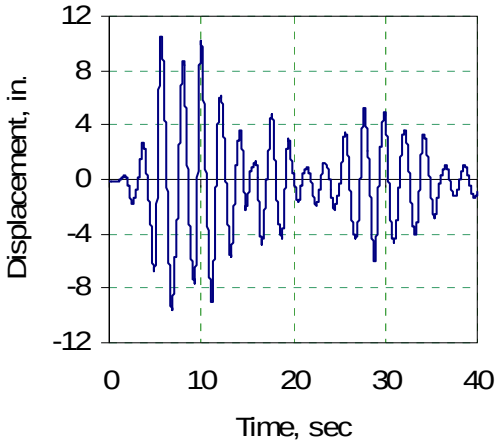

a. Roof displacement

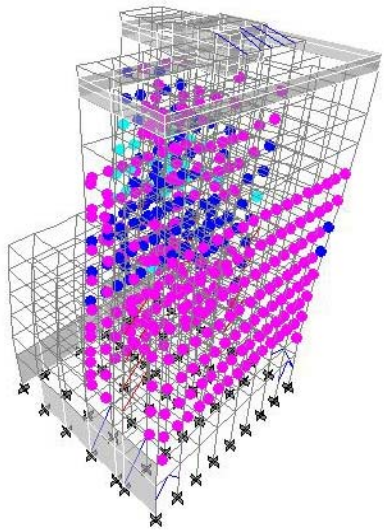

b. Hinge formation

Figure 14. Seismic demand and capacity, DBE level

Computer analyses typically do not capture the complete picture in regard to the building performance, and additional computations are frequently performed. Independent checks of concrete columns, beams, and beam-to-column joints were performed per ACI 318 [1] requirements. The calculations showed that the members had adequate shear capacity to resist the seismic demand at both DBE and MCE levels. The concrete joints we found to have adequate shear capacity to develop the probable plastic moment of the framing elements. The elements and connections attaching the damper and brace elements to the existing concrete framing were designed to transfer the forces at the MCE level. Finally, the FRP drag members were designed to transfer the MCE level forces. Given that: 1) the retrofitted building meets both the performance goals of LS at DBE and CP at MCE levels, 2) no non-ductile failure was anticipated, and 3) the retrofit components were designed for MCE level forces, the building met its performance objectives.

Figure 15 shows the normalized pushover curve for the building. The ordinates of roof displacement and base shear were normalized with respect to the building height and mass, respectively. The horizontal axis corresponds to an average drift ratio for the building and the vertical axis is its base shear coefficient (BSC). The DBE and MCE performance points are marked in the figure. The structure has substantial reserve capacity beyond the MCE demand. The analysis was carried up to a roof displacement of approximately 16 in. (400 mm)—significantly greater than the MCE target displacement of Figure 14. Although some of the plastic hinges in the concrete beams exceeded their CP level, the overall building response remained stable, as indicated by the non-degrading response illustrated in the figure.

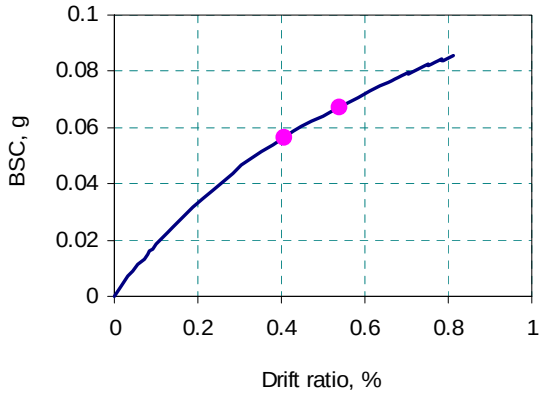

Figure 15. Normalized pushover curve

Table 3 presents the computed MCE drift ratios for the existing and retrofitted building obtained from the three-dimensional analyses. Only the drifts at the critical middle stories are shown. Note that the addition of dampers has reduced the story drifts by over 20%.

Floor	Existing	Retrofitted	Reduction, %
8	0.92	0.84	9
7	0.87	0.72	18
6	0.74	0.59	24
5	0.59	0.51	14

Table 3. Story drift reductions

FVDs increase the equivalent damping of the building by dissipating the seismic energy. Figure 16a presents the nonlinear force-displacement hysteresis for one of the FVDs during one of the MCE event. The FVD absorbs significant energy. Figure 16b shows the component of the seismic energy for the same event. For clarity, the data is normalized. The dampers dissipate approximately 75% of input seismic

energy. In the absence of the FVDs, the yielding of the existing concrete members would have been subject to this energy demand.

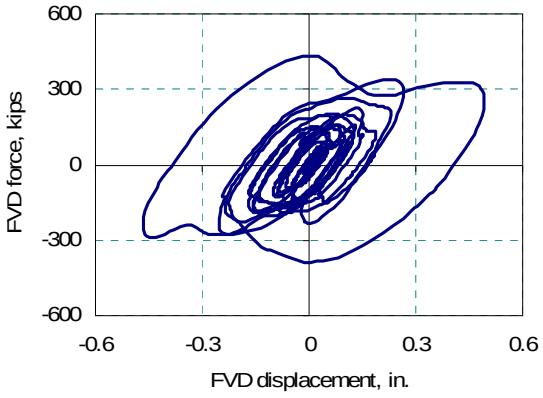

a. FVD response

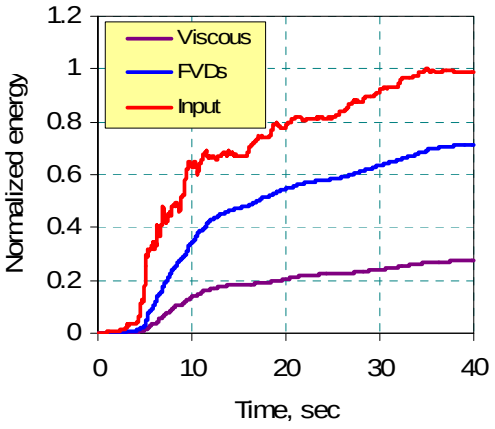

b. Components of seismic energy

Figure 16. Energy dissipated by FVDs for a typical acceleration history

Conclusions

State-of-the-art analysis of a historic reinforced concrete high-rise retrofitted with FVDs showed that the structure met its performance goals. Story drifts and member nonlinear actions were kept within the acceptable limits.

A. Performance-based earthquake engineering was effectively used to assess the seismic response of a historic reinforced concrete structure. This method readily identified a building weakness and the method to mitigate it.

B. FVDs provide an efficacious, cost-effective, and non-intrusive retrofit method. They act to increase the effective damping, do not stiffen the building, and reduce the seismic demand. The force in FVDs is primarily out-of-phase with elastic forces.

C. Steel HSS braces can be efficiently added to increase lateral stiffness and reduce torsional response resulting from un-even distribution of lateral-force resisting elements.

D. FRP can serve as collectors to transfer the seismic forces to the lateral force-resisting system and thus, eliminate the need to alter building configuration by adding concrete or steel beams.

E. In seismic retrofit design, additional analyses often need to be performed to guard against unforeseen failures not captured by the analytical model of the structure.

References

[1] ACI (2005), "ACI 318: Building Code requirements for structural concrete and commentary," American Concrete Institute, Farmington Hill, MI.

[2] Constantinou, M. and Symans, M. (1992), "Experimental & analytical investigation of seismic response of structures with supplemental fluid viscous dampers," Report No. NCEER-92-0032, University at Buffalo, State University of New York, Buffalo, N.Y.

[3] CSI (2006-1), "ETABS 9: Linear and nonlinear static and dynamic analyses and design of building systems," Computers and Structures Inc., Berkeley, CA.

[4] CSI (2006-2), "SAP Version 10, Linear and nonlinear static and dynamic analysis and design of three-dimensional structures," Computers and Structures Inc. Berkeley, CA.

[5] FEMA (2000), "FEMA 356: Prestandard and commentary for the seismic rehabilitation of buildings," Washington, D.C.

[6] Gilani A., Miyamoto, K., and Determan, L., (2006), Seismic rehabilitation of historic reinforced concrete buildings with fluid viscous dampers: two case studies, proceeding of the Eighth National Conference on Earthquake Engineering, San Francisco, CA.

[7] Singh, J.P. (2006), "Site Specific Time Histories for 926 J Street," Personal communications.

[8] Taylor Devices Inc. (2006), "Prototype tests of dampers for 926 J Street," Personal communications, Buffalo, New York.

[9] Wallace Kuhl (2005), "Material testing data for 926 J Street building," Personal communications.

[10] Chopra, A. (2001), "Dynamics of Structures: Theory and Applications to Earthquake Engineering," Prentice Hall, NJ.